ELSEVIER

Coordination Chemistry Reviews
219–221 (2001) 463–488

COORDINATION CHEMISTRY REVIEWS

www.elsevier.com/locate/ccr

Complexes with 2,2′-azobispyridine and related 'S-frame' bridging ligands containing the azo function

Wolfgang Kaim *

Institut für Anorganische Chemie, Universität Stuttgart, Pfaffenwaldring 55, D-70550 Stuttgart, Germany

Received 18 August 2000; received in revised form 17 January 2001; accepted 23 January 2001

Contents

Abstract

Bridging ligands involving the azo group –N=N– as coordinating π acceptor function can yield dinuclear complexes with unusual electronic and structural features. In particular, 2,2′-azobispyridine (abpy) as formally derived from the ubiquitous 2,2′-bipyridine ligand is now known to form a variety of complexes. The strong electronic interaction between the ligand and one or two metal centers was first noted in 1969 by Baldwin, Lever and Parish. Among the special properties of such systems are several easily accessible oxidation states,

* Tel.: +49-711-6854170/71; fax: +49-711-6854165.
E-mail address: kaim@iac.uni-stuttgart.de (W. Kaim).

0010-8545/01/$ - see front matter
PII: S0010-8545(01)00347-2

long-wavelength charge-transfer absorptions, relatively small metal–metal distances, various forms of isomerism, and the stability of radical intermediates and/or mixed-valent states.

Keywords: Azo compounds; Bridging ligands; Dinuclear complexes; Electronic structure; π Interaction

1. Introduction, aims and scope

In 1969 a paper by Baldwin, Lever and Parish [1] referred to an interesting unsaturated ligand, 2,2′-azobispyridine (abpy), which can conveniently be synthesized by oxidative coupling of 2-aminopyridine [2].

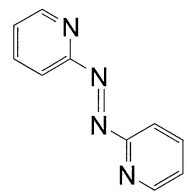

abpy

Although a report on copper(II) and cobalt(II) complexes with this ligand had appeared shortly before Ref. [3], the paper by Baldwin et al. made a particular point about: (i) the strong interaction of this ligand with metal ions, especially with low-spin iron(II); and (ii) the potential for several different coordination modes (mono- and dinuclear) according to Scheme 1 [1].

As will be specified in this review (Section 3), the structurally established alternatives include the mono- and dinuclear coordination situations **I** and **IIb** with five-membered chelate ring formation NNCNM.

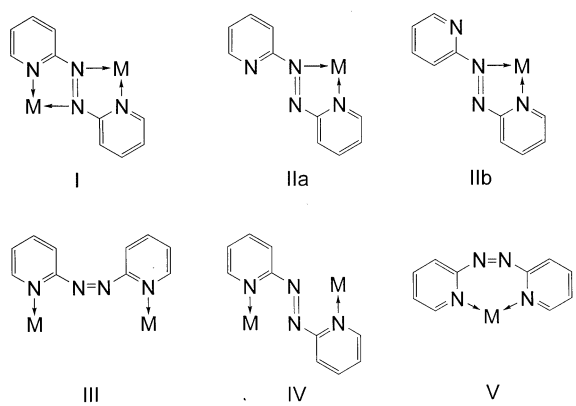

Scheme 1.

Azoaromatic compounds have been increasingly studied in materials chemistry because of their unique combination of geometrical and electronic structures [4,5]. The low-lying azo-centered π* molecular orbital is responsible for the intense long-wavelength absorption (dye function) and the non-linear optical properties (information storage function). In addition, this chromophore can undergo a photoinduced Z/E isomerization [4] and is suitable for modifications to form mesogenic films or polymers [5]. The low-lying π* MO may also be directly populated by one or two electrons, chemically or electrochemically. The resulting two-step redox system (Scheme 2) contains a radical anion as an intermediate and a 1,2-disubstituted hydrazido(2-) species as fully reduced form.

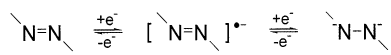

Scheme 2.

The coordination chemistry of azo (diazene) compounds in general has long been relevant for dye development [6] and nitrogen fixation. Selected aspects have been reviewed [7,8]. It is the purpose of this article to summarize the characteristics of the abpy ligand and of some related systems. Abpy is *formally* related to the ubiquitous 2,2′-bipyridine through the insertion of the azo group between the two pyridyl moieties.

Among the azo ligands there are monodentate and bidentate (chelating) examples such as the continuously studied [9,10] and reviewed [11] 2-phenylazopyridine (pap) ligands, which have been known for some time as excellent π acceptors and even stable radical ligands [12,13]. In fact, the mononuclear complexes of abpy (which will also be presented in this review) are quite similar to analogous compounds with pap ligands. Considering the dominating electronic influence of the azo group (vide infra) the replacement of phenyl by pyridyl substituents has rather little effect. However, abpy is not simply another such azo ligand, its ability to bridge *two* metal centers at a distance of about 5 Å via edge-sharing of two five-membered chelate rings, the small size of its π system and the low-lying π* orbital [14] make it a very special ligand, suitable for studying metal–metal interaction across an unsaturated bis-chelating [14] molecular bridge. Such ligands have become important for studies of intramolecular electron transfer [15], magnetic coupling [16] and mixed-valence chemistry [17].

2. Survey of abpy complexes

Well-characterized coordination compounds of the abpy ligand are known for several transition metals and for tin(IV) complex fragments. Table 1 summarizes the reported systems together with the kinds of studies performed.

It is obvious from Table 1 that metal centers with d^6 configuration feature prominently in the coordination chemistry of the abpy ligand, largely because of the good match between the π* acceptor MO of abpy and the dπ orbitals of the

Table 1
Survey of studies on abpy and its metal complexes

abpy	X-ray [18]; ^{1}H-NMR (*cis*/*trans* isomers) [19]; IR, Raman [20]; CV, UV–vis [21–23]; UV–vis spectroelectrochemistry [19]; ESR (red) [24,25]; calculations [18,19]
$(abpy)Cr^{0}(CO)_4$	CV, IR, UV–vis [14]
$\{(\mu\text{-abpy})[Cr^{0}(CO)_4]_2\}^{\bullet -}$	ESR [24]
$(abpy)Mo^{0}(CO)_4$	X-ray [26]; ^{1}H-NMR [14]; ^{95}Mo-NMR [27]; CV, IR, UV–vis [14,23,28,29]; solvatochromism [30]
$(\mu\text{-abpy})[Mo^{0}(CO)_4]_2$	^{1}H-NMR, CV, IR, UV–vis–NIR [14,23,28,29]; solvatochromism [30]; ESR (red) [24]; ENDOR (red) [24]
$\{(\mu\text{-abpy})[W^{0}(CO)_4]_2\}^{\bullet -}$	ESR [24,25]
$(abpy)Re^{I}(CO)_3Cl$	X-ray, ^{1}H-NMR, CV, IR, UV–vis, IR-, UV–vis spectroelectrochemistry, ESR (red) [31]
$(abpy)Re^{I}(CO)_3X$, X = Br, CF_3SO_3 [a]	CV, IR, UV–vis, IR-, UV–vis spectroelectrochemistry [32]
$(\mu\text{-abpy})[Re^{I}(CO)_3Cl]_2$	X-ray (*trans* isomer) [31]; ^{1}H-NMR, CV, IR, UV–vis–NIR, IR-, UV–vis–NIR-spectroelectrochemistry [31,33]; ESR (red) [25,33]
$(\mu\text{-abpy})[Re^{I}(CO)_3Br]_2$	CV, IR, UV–vis–NIR [31,33]; UV–vis–NIR-spectroelectrochemistry [33]; ESR (red) [25,33]
$(abpy)_2Fe^{II}(NCS)_2$	IR, UV–vis [1]
$[(abpy)Fe^{II}(CN)_4](X)_2$, X = K, NBu_4	CV, IR, UV–vis, ESR (ox/red) [34]
$[(abpy)Ru^{II}(bpy)_2](PF_6)_2$	CV, UV–vis [19,35]; UV–vis spectroelectrochemistry [19]; ESR (red) [19,36]; calculations [37]
$\{(\mu\text{-abpy})[Ru^{II}(bpy)_2]_2\}(PF_6)_4$ [b,c]	^{1}H-NMR [38]; isomerism [38,39]; CV, UV–vis–NIR [19,23,35,38,39]; UV–vis spectroelectrochemistry (6 red, 1 ox) [19,38,43]; ESR (red) [25,36]
$\{(\mu\text{-abpy})\ [Ru^{II}(4,4'\text{-}Me_2bpy)_2]_2\}(PF_6)_4$ [b,c]	^{1}H-NMR, isomerism, CV, UV–vis–NIR, UV–vis spectroelectrochemistry (6 red, 1 ox) [38]
$[(abpy)_3Ru^{II}](PF_6)_2$	X-ray (*mer* isomer) [40]; ^{1}H-NMR [19]; CV, UV–vis [19,35,42]; UV–vis spectroelectrochemistry [19]; ESR (red) [19,36]; calculations [37]
$(abpy)_2Ru^{II}Cl_2$	X-ray (*ctc* isomer) [40]; CV, IR, UV–vis [42]
$[(abpy)_2Ru^{II}X_2](ClO_4)_n$ [d]	CV, IR, UV–vis [42]
$[(abpy)_2(bpy)Ru](PF_6)_2$ (3 isomers) [e]	^{1}H-NMR, CV, UV–vis, UV–vis spectroelectrochemistry, ESR (red) [19,41]; calculations [37]
$(abpy)_2Os^{II}Cl_2$	X-ray (*ctc* isomer [43])
$\{(\mu\text{-abpy})[Ru^{II}(bpy)_2][Os^{II}(bpy)_2]\}(PF_6)_4$	^{1}H-NMR, CV, UV–vis–NIR, UV–vis–NIR spectroelectrochemistry (4 red, 1 ox), ESR (red/ox) [43]
$\{(\mu\text{-abpy})[Os^{II}(bpy)_2]_2\}(PF_6)_4$	^{1}H-NMR, CV, UV–vis–NIR, UV–vis–NIR spectroelectrochemistry (4 red, 1 ox), ESR (red) [43]
$[(abpy)Os^{II}(C_6Me_6)Cl](PF_6)$	^{1}H-NMR, CV, UV–vis–NIR, UV, spectroelectrochemistry (2 red), ESR (red) [44]
$\{(\mu\text{-abpy})[Os^{II}(C_6Me_6)Cl]_2\}(PF_6)_2$	^{1}H-NMR, CV, UV–vis–NIR, UV–vis–NIR spectroelectrochemistry (3 red) [44]
$\{(\mu\text{-abpy}^{\bullet -})[Os^{II}(C_6Me_6)Cl]_2\}(PF_6)$	ESR (red) [f] [44]
$(abpy)Co^{II}Cl_2$	UV–vis, magnetism [3]
$(abpy)_2Co^{II}Cl_2$	IR, UV–vis, magnetism [1,3]
$(abpy)_2Co^{II}Br_2$	IR, UV–vis, magnetism [1]
$(abpy)_2Co^{II}(NCS)_2$	IR, UV–vis, magnetism [1]
$(\mu\text{-abpy})[Co^{II}(hfacac)_2]_2$	T-dependent magnetism [26]

Table 1 (*Continued*)

(μ-abpy)[$Co^{II}Cl_2$]$_2$	IR, UV–vis, magnetism [1,3]
(μ-abpy) [$Co^{II}(SO_4)$]$_2$	UV–vis, magnetism [3]
(abpy)$Rh^{I}(C_5Me_5)$	^{1}H-NMR, CV, UV–vis [45]
[(abpy)$Rh^{III}(C_5Me_5)Cl](PF_6)$	^{1}H-NMR, CV, UV–vis, UV–vis–NIR spectroelectrochemistry, ES R (red) [45]
{(μ-$abpy^{\cdot -}$[$Rh^{III}(C_5Me_5)$-Cl]$_2$}(PF_6)	CV, UV–vis, UV–vis–NIR spectroelectrochemistry, ESR [45]
(abpy)$Ir^{I}(C_5Me_5)$	^{1}H-NMR, CV, UV–vis [45]
[(abpy)$Ir^{III}(C_5Me_5)Cl](PF_6)$	^{1}H-NMR, CV, UV–vis, UV–vis–NIR spectroelectrochemistry, ESR (red) [45]
{(μ-abpy)[$Ir^{III}(C_5Me_5)Cl]_2$}$(PF_6)_2$	CV, UV–vis, UV–vis–NIR spectroelectrochemistry [45]
{(μ-$abpy^{\cdot -}$[$Ir^{III}(C_5Me_5)Cl]_2$}(PF_6)	CV, UV–vis, UV–vis–NIR spectroelectrochemistry, ESR [45]
(abpy)$_2Ni^{II}(NCS)_2$	IR, UV–vis, magnetism [1]
[(abpy)$_3Ni^{II}](ClO_4)_2$	IR, UV–vis, magnetism [1]
(μ-abpy)[$Cu^{I}X]_2$, X = Cl, I	IR, UV–vis [1]
{(μ-abpy)[$Cu^{I}(PPh_3)_2]_2$}$(BF_4)_2$	X-ray [26]; CV, UV–vis–NIR, UV spectroelectrochemistry, ESR (red) [46a]
{(μ-abpy)[$Cu^{I}(X)_2]_2$}$(BF_4)_2$ [g]	CV, UV–vis–NIR, UV spectroelectrochemistry, ESR (red) [46a]
{(μ-$abpy^{\cdot -}$)[$Cu^{I}(Ph_2P(CH_3)_6$-$PPh_2)]_2$}(BF_4)	ESR (245 GHz) [46b]
(abpy)$Cu^{II}X_2$, X = Cl, Br	UV–vis, magnetism [3]; IR, Raman [20]
(abpy)$_2Cu^{II}X_2$, X = Cl, Br	UV–vis, magnetism [3]; IR, Raman [20]
(abpy)$_2Cu^{II}(NCS)_2$	IR, UV–vis, magnetism [1]
(μ-abpy)[$Cu(OAc)_2]_2$	IR, UV–vis, magnetism [1]
(μ-abpy)[$Cu^{II}Cl_2]_2$	IR, Raman, UV–vis, magnetism [1,3,20]
(μ-abpy)[$Cu^{II}Br_2]_2$	UV–vis, magnetism [3]; IR, Raman [20]
(μ-abpy) [$Cu^{II}(SO_4)$]$_2$	UV–vis, magnetism [3]
(abpy)$Zn^{II}(X)_2$ [h]	IR, Raman [20]
(abpy)$Sn^{IV}Br_2(CH_3)_2$	X-ray, Mössbauer, XPS [47]
(abpy)$Sn^{IV}X_nR_{4-n}$ [i]	IR [48]; Mössbauer, XPS [47]

[a] X = THF or PPh_3 through in situ substitution.
[b] Separate data for *meso* and *rac* complexes in Ref. [38].
[c] Analogous complexes with 4,4′-dimethyl-2,2′-azobispyridine [38].
[d] X = H_2O, CH_3CN, C_5H_5N ($n = 2$); X = Br, NO_2 ($n = 0$).
[e] Separate data for *cct*, *ctc* and *ccc* isomers [19,41].
[f] X and W band measurements.
[g] X = $Ph_2P(CH_2)_nPPh_2$, $n = 2$, 5 and6
[h] X = Cl, Br, I, NCS, NO_3.
[i] X = Cl, Br; R = Me, *n*-Bu, *n*-Oct; $n = 2$–4.

low-valent d^6 centers. The capability of abpy to act as a metal–metal bridging ligand (μ-abpy) or as a radical anion ($abpy^{\cdot -}$) is also illustrated in Table 1.

3. Structural aspects

All structurally established coordination compounds of abpy have the ligand bonded to one or two metal centers via the azoimine (N=N–C=N) chelate arrangement. This situation, illustrated by structures **I** or **IIa** and **b** from Scheme 1, creates

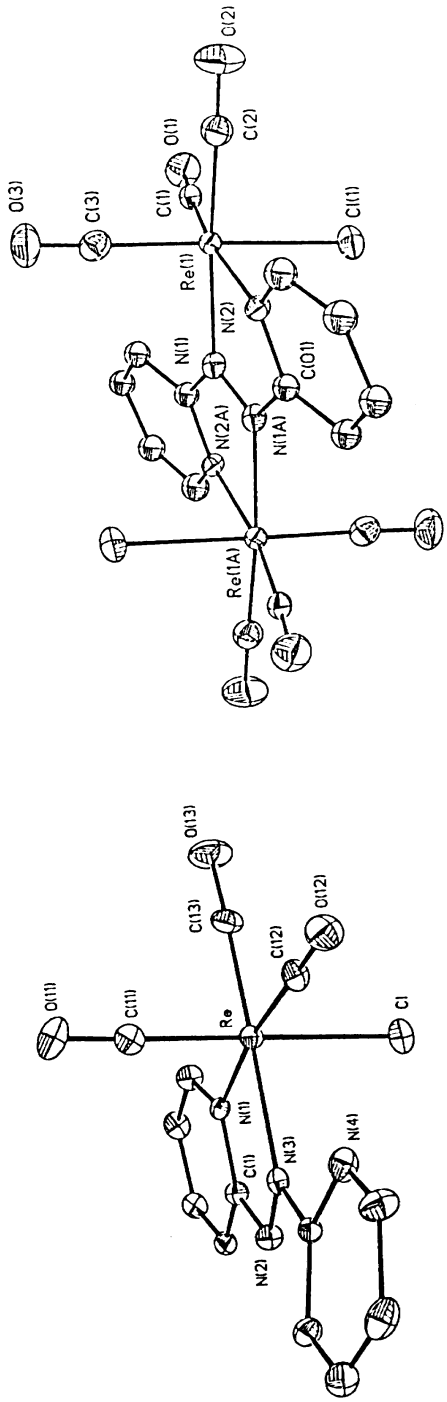

Fig. 1. Molecular structures of (abpy)$Re(CO)_3Cl$ and (μ-abpy)$[Re(CO)_3Cl]_2$ (from Ref. [31]).

energetically favorable five-membered chelate rings that are generally preferable to seven-membered alternatives such as **V** [1]. Non-chelate bonding of bis-monodentate abpy (structures **III** and **IV**) is conceivable but has not yet been documented. While **I**, **IIa,b** and **IV** have the *E* (*trans*) configuration at the azo function, alternatives **III** and **V** must adopt the higher energy *Z* (*cis*) configuration. For the free ligand, both configurations can be distinguished by NMR [19].

The conformation of the free 2-pyridyl rings is another source of structural variety. In metal-free crystallized abpy the *s-trans*/*E*/*s-trans* arrangement as depicted in the initial formula is observed for the coplanar molecule [18]. In solution or in the gas phase the energy minimum conformation may be different [19], as suggested by PM3 calculations [18]; repulsion effects between azo-N lone pairs and the *ortho*-CH or pyridyl-N lone pairs and contributions from π conjugation combine to create a complex energy hypersurface [18].

Formation of a mono-chelate complex creates structural alternatives **IIa** and **IIb** for the remaining free 2-pyridyl ring. The X-ray analysis data available for $(abpy)Mo(CO)_4$ [26], $(abpy)Re(CO)_3Cl$ [31], $[(abpy)_3Ru](PF_6)_2$ [40] and $(abpy)_2MCl_2$, M = Ru [40], Os [43], and $(abpy)SnBr_2(CH_3)_2$ [47] come close to situation **IIb** with the pyridyl-N directed toward the chelated metal atom (Fig. 1). Distances of more than 3.0 Å and a close to octahedral coordination rule out any additional bonding interaction to the transition metals with their d^6 configuration. Instead, the 2-pyridyl twist (Scheme 3) from conformation **IIa** to conformation **IIb** minimizes the non-bonding contacts between the ancillary ligands on M and the pyridyl group (**IIb**: N lone pair; **IIa**: CH bond).

Such interactions must inevitably occur for dinuclear species such as (μ-abpy)$[Re(CO)_3Cl]_2$ [31], where a twist of μ-abpy of 17.7° serves to diminish the repulsion (Fig. 1). Unusual ^{1}H-NMR shifts for the $H^{3,3'}$ protons in the dirhenium(I) and dimolybdenum(0) carbonyl complexes reflect this intramolecular contact [14,31]. For d^{10} species such as $\{(\mu\text{-abpy})[Cu(PPh_3)_2]_2\}^{2+}$ with an approximately tetrahedral configuration at the metal centers such repulsive interactions in the abpy plane are absent [26]. In contrast to the mononuclear transition metal compounds mentioned, compound $(abpy)SnBr_2(CH_3)_2$ [47] with its large main group metal center exhibits three bonding distances Sn–N between 2.585(17) and 2.899(17) Å. Although the latter (between tin(IV) and the extra pyridyl–N) is rather long, the approximately pentagonal bipyramidal coordination geometry suggests a tridentate abpy ligand for this species [47].

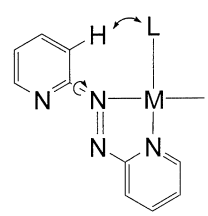

Scheme 3.

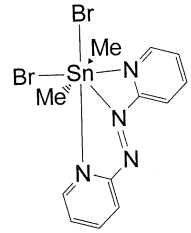

In contrast to the related π acceptor chelate systems of 1,4-diazabutadienes [49,50] and tetraazadienes [51], the unsymmetrical azoimine (here: azo-2-pyridyl) function allows for different bonding of metal centers to the significantly different donors of the bidentate ligand. Whereas the pyridyl rings are relatively basic (but poorly π accepting), the azo nitrogen centers are not; azobenzene has $pK_{BH^+} = -2.93$ [52]. Nevertheless, the superior π acceptor capability of azo nitrogen atoms can well compensate for that low basicity; in effect, the metal centers in (abpy)-$Mo(CO)_4$ [26], (abpy)$Re(CO)_3Cl$ [31], $[(abpy)_3Ru](PF_6)_2$ [40], $(abpy)_2MCl_2$, M = Ru [40] and Os [43], (μ-abpy)$[Re(CO)_3Cl]_2$ [31] and $\{(\mu\text{-abpy})[Cu(PPh_3)_2]_2\}^{2+}$ [26] are bonded at rather similar distances ($\Delta d < 0.07$ Å) by the azo-N and pyridyl-N donor atoms (Table 2). The special tridentate coordination of abpy in (abpy)$SnBr_2(CH_3)_2$ [47] is probably responsible for a short Sn–N(azo) bond of 2.585(17) Å and the longer Sn–N(pyridyl) bonds of 2.793(18) and 2.899(17) Å.

The 'S-frame' conformation s-*cis*/*E*/s-*cis* of abpy in dinuclear complexes with two five-membered chelate rings sharing a common side allows for a rather short intramolecular metal–metal distance in the absence of direct or atom-bridged metal–metal interactions. The two characterized examples (μ-abpy)$[Re(CO)_3Cl]_2$ [31] and $\{(\mu\text{-abpy})[Cu(PPh_3)_2]_2\}(BF_4)_2$ [26] exhibit distances of 5.033 and 4.937 Å, respectively (Table 2). These distances are thus considerably shorter than those in dinuclear systems bridged by more conventional ligands such as 2,2′-bipyrimidine (ca. 5.6 Å) [53,54] or pyrazine (ca. 6.9 Å) [55]. They are even shorter than in dinitrogen-bridged compounds [56] due to the twisting illustrated in Scheme 4.

At those metal–metal distances ancillary bidentate ligands like $Ph_2P(CH_2)_nPPh_2$ of medium chain length ($n = 5$ and 6) may act as bridging, instead of chelating, ligands [46a,54].

The asymmetry of the five-membered chelate rings formed by abpy and its capability to bind two metal centers allows for several kinds of isomerism in complexes with octahedral metal centers. The tris(2,2′-azobipyridine)ruthenium(II) dication exists as *fac* and *mer* isomers. The latter could be crystallized and thus, independently identified [40]. Species $[(abpy)_2MX_2]^{n+}$, M = Ru or Os, X_2 = *cis*-Cl_2

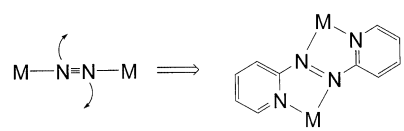

Scheme 4.

($n = 0$) or 2,2′-bipyridine ($n = 2$), can exist in three configurations [11,19,40,41] as depicted in Fig. 2, as *ctc*, *cct* (both C_2 symmetry) and *ccc* (C_1) isomers. (*c* for *cis* and *t* for *trans* denote the relations between Cl, N(2-pyridyl) and N(azo) donor atoms, in that order).

Two further isomers *ttt* (C_{2h}) and *tcc* (C_{2v}) would be expected for $(abpy)_2MCl_2$ with chloride ligands in *trans* position. All three isomers $[(abpy)_2Ru(bpy)](PF_6)_2$ were separated and characterized (Table 1) [19,41]; they exhibit unusually strong differences of intramolecular electron transfer when reduced (cf. Section 7) [41]. The *ctc* isomers $(abpy)_2MCl_2$, M = Ru and Os, which are precursor materials for the above complexes with bpy were structurally characterized (Fig. 3) [40,41].

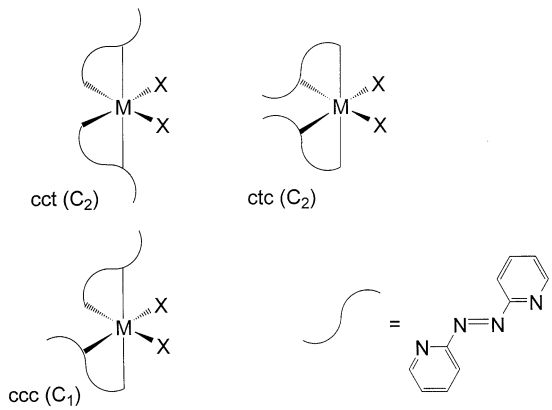

Fig. 2. Isomers of molecules $(abpy)_2MX_2$ with ligands X_2 in *cis* configuration (e.g. $X_2 = Cl_2$ or bpy): *c* for *cis* and *t* for *trans* indicate the relations between X, N(2-pyridyl) and N(azo) donor atoms.

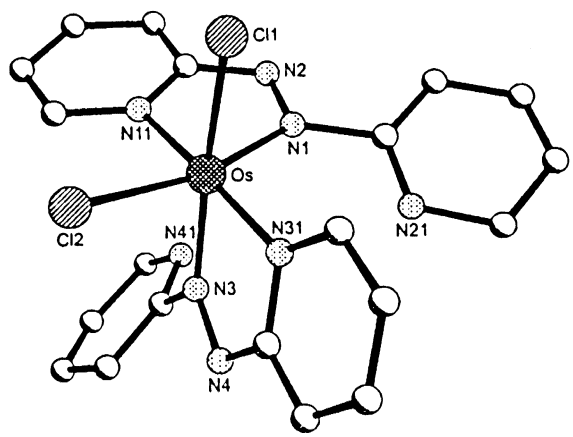

Fig. 3. Molecular structure of *ctc*-$(abpy)_2OsCl_2$ [43b].

Positional isomerism in dinuclear complexes of abpy can occur for instance in (μ-abpy)[$Re(CO)_3Cl]_2$. The preference of the carbonyls for a *fac* arangement leaves a *cis* or *trans* arrangement possible for the chloride ligands, relative to the abpy plane (Scheme 5) [33]. Only one isomer has been detected by ^{1}H-NMR, which was identified as the *trans* alternative [31].

The absence of a center or plane of symmetry for the individual metal sites in complexes such as $\{(\mu\text{-abpy})[Ru(bpy)_2]_2\}^{4+}$ allows for the existence of two diastereomers, a pair of ΔΔ/ΛΛ enantiomers and the meso form (ΔΛ) (Fig. 4) [38,39]. A detailed study of the latter with abpy or its 4,4′-dimethyl derivative and with bpy or its 4,4′-dimethyl form has shown that the separated and NMR-spectroscopically identified diastereomers clearly exhibit differences in their metal–metal interactions [38].

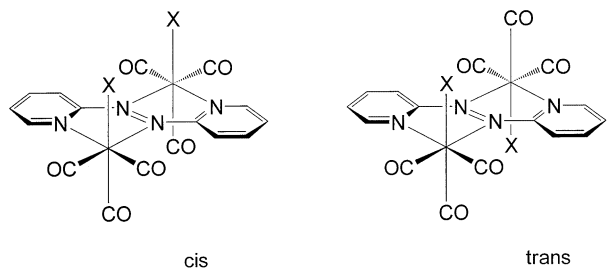

Scheme 5.

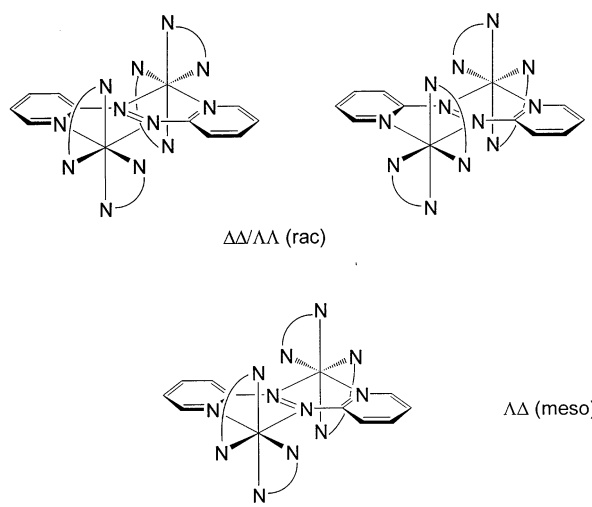

Fig. 4. *Meso* and *rac* isomers of complex ions $\{(\mu\text{-abpy})[M(N\,\hat{}\,N)_2]_2\}^n$ [39].

4. Electronic structure of the ligand

Before discussing the various experimental manifestations of the unusual ligand effects of abpy some fundamental MO properties will be reviewed. Hückel MO (HMO [14,24]) as well as more sophisticated calculations [19] agree in postulating a particularly stabilized lowest unoccupied MO (LUMO, b_g) for abpy. This π^* acceptor orbital is mainly, but not exclusively, centered on the azo function (Fig. 5); the pyridyl nitrogen centers also contribute, as is evident from the EPR/ENDOR coupling constants (cf. Section 7 below [24]). Taken together, however, the four coordinating nitrogen centers of abpy account for about two-thirds of the orbital coefficients of the LUMO — an unusually large value that correlates e.g. with the strong metal coordination effects on the reduction potential, the high charge transfer absorption intensities [14] and the facile protonation after reduction [19].

The second lowest unoccupied MO (SLUMO, a_u) has quite a different character and lies at far higher energies, together with another unoccupied π MO of b_g symmetry. HMO perturbation calculations [14] confirm that metal coordination strongly stabilizes the LUMO further.

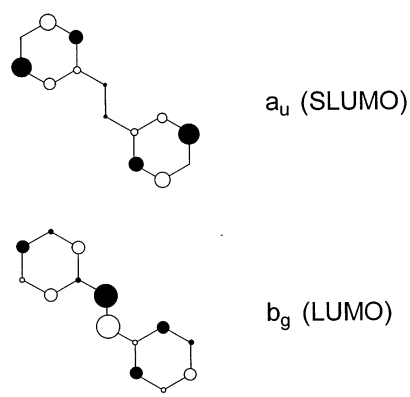

Fig. 5. Lowest unoccupied π molecular orbitals of abpy (from Hückel MO calculations; $h_N = 0.8$ [14]).

5. Electrochemistry

At -1.37 V versus the ferrocene/ferrocenium couple (DMF, 198 K) the reduction potential of abpy [19] is just about 0.3 V more negative than that of typical quinones [57]. Compared to bpy (-2.55 V [19]) the reduction is facilitated by more than 1 V.

The large contributions of the coordinating N centers, in particular of the azo atoms, to the LUMO (Fig. 4) are responsible for the additional stabilization of the reduced forms of abpy on coordination with one or two metal centers. As an example, (abpy)$Re(CO)_3Cl$ is reduced at -0.78 V and the dinuclear (μ-

abpy)[Re(CO)$_3$Cl]$_2$ at 0.00 V versus $(H_5C_5)_2Fe^{0/+}$ [31]. It is not surprising, therefore, that some of the dinuclear complexes are already obtained as reduced (radical) species from the reaction mixtures [31,44–46].

The difference between the first and second one-electron reductions lies at about 0.6 V for abpy and its complexes [14,19], which compares with much higher values for 1,2,4,5-tetrazine-based bridging ligands [14,58].

Further reduction that occurs e.g. for $\{(\mu\text{-abpy})[Ru(bpy)_2]_2\}^{4+}$ was initially attributed in part to $abpy^{3-/4-}$ [19]. However, a detailed differential pulse voltammetric study on derivatives and isomers has later shown that all bpy co-ligands are first reduced to the anionic state (Scheme 6) [38].

The study of individual diastereomeric forms of $\{(\mu\text{-abpy})[Ru(bpy)_2]_2\}^{4+}$ and of related species [38] has shown that *meso* and *rac* isomers differ slightly (0–45 mV) in their redox potentials.

Although the radicals $(abpy^{\cdot -})[Re(CO)_3X]_{1,2}$ are quite persistent [25,31–33], such rhenium(I) complexes of abpy slowly lose the halide after the second-electron uptake [31,32]. A detailed IR-spectroelectrochemical study has yielded the following sequence for (abpy)Re(CO)$_3$X, X = Br or OTf, [32], involving a total of three added electrons (Scheme 7).

On the oxidative side, the low-lying π* MO of abpy makes this ligand a potent bridge for d^5–d^6 mixed-valent pairs of metal centers [39]. As a well-researched

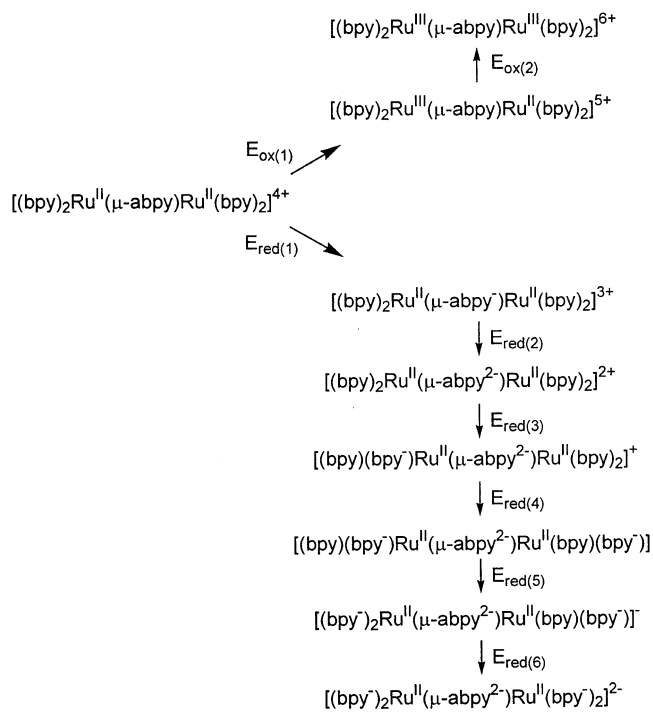

Scheme 6.

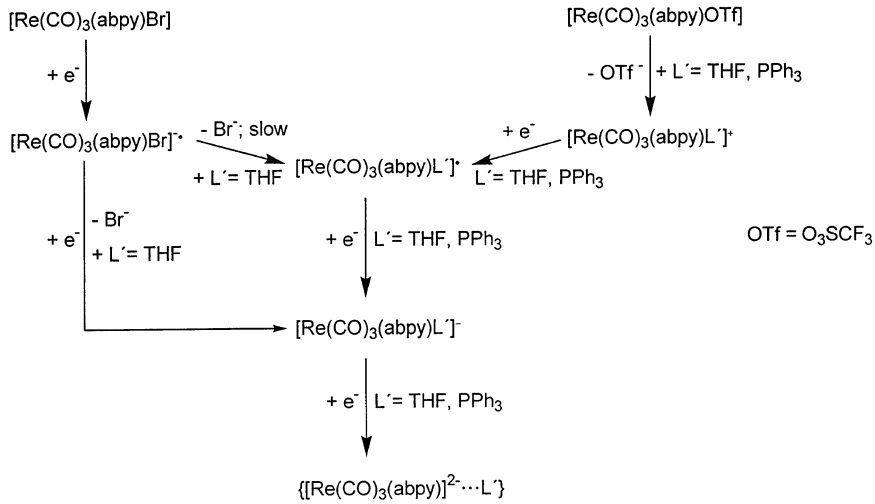

Scheme 7.

example [19,38,39,43], the stepwise metal-centered one-electron oxidation of $\{(\mu\text{-abpy})[Ru(bpy)_2]_2\}^{4+}$ occurs with about 0.5 V potential separation, which translates to comproportionation constants K_c of 10^8–10^9 [19,38,39].

$$K_c = 10^{\Delta E/59\ mV} = [M^{(n+1)}]^2/[M^n][M^{(n+2)}] \quad (1)$$

$$M^n + M^{(n+2)} = 2M^{(n+1)}$$

Other bridging ligands such as 2,2′-bipyrimidine or 2,5-di(2′-pyridyl)pyrazine induce much lower K_c values for the dinuclear $(bpy)_2Ru^{2+/3+}$ system [39]. The mediating function of the π*(abpy) acceptor orbital is further supported [59] by the fact that the diosmium analogue $\{(\mu\text{-abpy})[Os(bpy)_2]_2\}^{4+}$ has $K_c > 10^{17}$ [43].

The facile reduction of abpy, especially when coordinated, has allowed us to break up two-electron ECE or EEC processes that occur in the reductive dehalogenation of complexes $[(N \wedge N)MCl(C_nR_n)]^+$ (M = Rh, Ir and $n = 5$; M = Os and $n = 6$) [60–62]. These reactions produce coordinatively unsaturated intermediates $(N \wedge N)M(C_nR_n)$ for eventual hydride transfer catalysis [62–64]. With N ^ N = bpy and related ligands there are only electrochemically irreversible two-electron processes observed, even at fast scan rates [60–64]. With abpy, however, a one-electron intermediate $[(N \wedge N)MCl(C_nR_n)]^{\bullet}$ is detectable through cyclic voltammetry and spectroelectrochemistry (UV–vis, EPR) [44,45]. Thus, abpy proves an interesting pendant to bpy and related, more commonly used ligands in catalysis, photo- or electrochemistry.

As in the pure electron transfer situation mentioned above for systems $\{(\mu\text{-abpy})[M(bpy)_2]_2\}^{n+}$ (M = Ru and Os), the abpy bridging ligands induces a large splitting of potentials for the bond-breaking in complexes $\{(\mu\text{-abpy})[MCl(C_nR_n)]_2\}^k$

(M = Rh, Ir and $n = 5$; M = Os and $n = 6$) [44,45]. Both the closeness (ca. 5 Å) of the reaction centers (Coulombic interaction) and the strong electronic coupling through the azo bridge contribute to this effect.

The localization of the added electrons in the azo function of abpy produces an unusually large splitting of redox potentials in $[(abpy)_2Ru(bpy)]^{2+}$ and $[(abpy)_3Ru]^{2+}$ [19,35]. This strong Coulombic effect [65] in the case of abpy can be attributed to strong ligand–ligand coupling via the central metal and/or to significant geometrical reorganization following the electron uptake [35].

6. Spectroscopy and spectroelectrochemistry (UV–vis–IR)

The low-lying LUMO (b_g) of abpy with its MO coefficients centered largely at the four coordinating nitrogen centers is ideally suited for π back donation from chelated low-valent metal centers, especially for d^6, d^8 and d^{10} configurations.

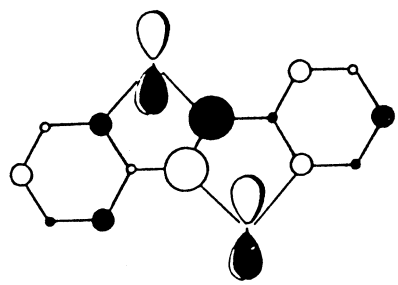

The very low energy of the π*(abpy) MO, especially after the second metal coordination, is responsible for the long-wavelength metal-to-ligand charge transfer (MLCT) bands. These are usually in the visible for mononuclear complexes [1,14,19,23,31,35,42,44,45] and frequently in the near infrared (NIR) for dinuclear systems [14,19,23,33,35,38,43–46]. For instance, the molybdenum(0) complexes $(abpy)Mo(CO)_4$ and $(\mu\text{-abpy})[Mo(CO)_4]_2$ absorb in THF solutions at 620 and 900 nm, respectively [14]; dicopper(I) compounds have their absorption maximum at lower wavelengths, at 611 nm for $(\mu\text{-abpy})[CuCl_2]_2$ [1] or 700 nm for $\{(\mu\text{-abpy})[Cu(Ph_2P(CH_3)_6PPh_2)]_2\}(BF_4)_2$ (Fig. 6) [46].

The intensities of these MLCT ($d\pi \rightarrow \pi^*$) bands are typically high because of the large LUMO coefficients at the coordinating nitrogen centers, the 'ligand-to-metal interface' [14]. At the same time, the relatively strong mixing of abpy π* and metal dπ orbitals as calculated for ruthenium(II) systems [37] produces fairly narrow MLCT bands [14]. The first, intense MLCT band is usually well separated from additional MLCT features at higher energies that involve higher-lying unoccupied MOs; the large energy difference between the LUMO (b_g) and the SLUMO (a_u) has been referred to in Section 4 [14]. Summarizing, the low transition energy, high intensity, small bandwidth and large separation from the next MLCT absorptions render the complexes of abpy with low-valent metals ideal test systems to study metal-to-ligand charge transfer. For instance, the individual diastereomeric *meso*

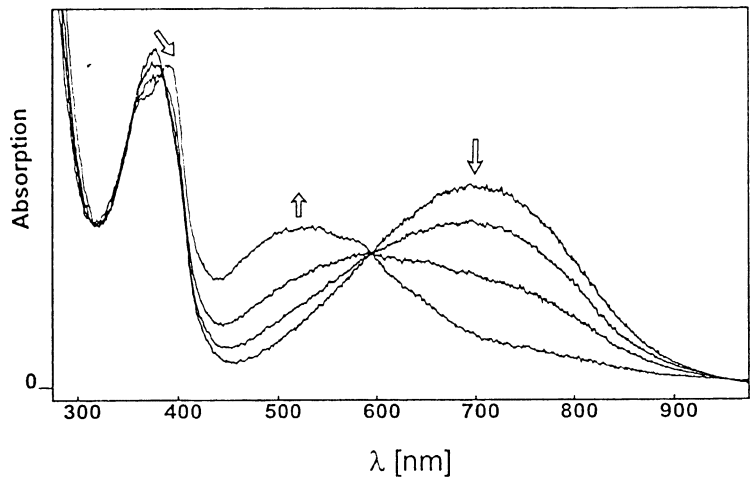

Fig. 6. UV–vis spectroelectrochemistry of $\{(\mu\text{-abpy})[Cu(Ph_2P(CH_2)_6PPh_2)]_2\}^{(2+)\rightarrow(\bullet+)}$ in CH_2Cl_2/0.1 M Bu_4NPF_6 [46a].

and *rac* forms of $\{(\mu\text{-abpy})[Ru(bpy)_2]_2\}^{4+}$ and of related species differ slightly but perceptibly (ca. 6 nm) in their absorption energies [38].

Generally, the MLCT bands of abpy complexes exhibit relatively little solvatochromism, in agreement with the significant metal–ligand orbital mixing [37]. On MLCT excitation, the transition moment is directed opposite to the ground state polarization $M^{\delta-}$–$L^{\delta+}$, which typically reduces the dipole moment of the excited state and thus produces hypsochromic shifts in solvents of higher 'polarity' (negative solvatochromism). Unexpectedly, a stronger solvent sensitivity was observed for the centrosymmetric dinuclear $(\mu\text{-abpy})[Mo(CO)_4]_2$ in comparison to the mononuclear $(abpy)Mo(CO)_4$ [30]. Polarizability differences for the whole molecules [30] have been proposed to account for this effect; an alternative model proposed by Lever and Dodsworth involves local solvation effects (dipole–dipole interactions) at the individual polar metal–ligand interfaces [66].

The high amount of metal-to-abpy π back donation in the corresponding complexes with electron-rich metal centers is evident not only from the diminished solvatochromism [30] but also from the hypsochromically shifted MLCT transitions from ruthenium(II) to the ancillary bpy ligands in $\{(\mu\text{-abpy})[Ru(bpy)_2]_2\}^{4+}$ [35]. IR vibrational spectroscopy also provides evidence for this strong interaction, either through the vibrations of abpy itself [1] or, indirectly, through the analysis of CO stretching frequencies in coordinated carbonylmetal fragments [14,31,32].

In view of the multi-step electron transfer reactivity of many coordination compounds of abpy (cf. Schemes 6 and 7) IR and UV–vis–NIR spectroelectrochemical techniques have often been used to identify and characterize the corresponding intermediates (Fig. 6) [19,31–33,38,43–46]. The ligand itself exhibits a high-energy shift of the $n\rightarrow\pi^*$ band and a bathochromic shift of the HOMO–LUMO transition on reduction, while new low-energy transitions at about 400–500 nm occur, originating from the singly or doubly occupied b_g MO [19]. Such

transitions are also observed for the coordinated species where the long-wavelength MLCT band is typically shifted to much higher energies [19,31,38].

Spectroelectrochemistry was also used to generate species (abpy)M(C_nR_n) and (μ-abpy)[M(C_nR_n)]$_2$ (M = Rh, Ir, $n = 5$; M = Os, $n = 6$) with formally d^8 configured metal centers [44,45]. The dinuclear systems show intense absorptions at very long wavelengths (ca. 1000 nm).

7. EPR of paramagnetic species

The facile one-electron reduction of abpy and its metal complexes has prompted investigations of coordination compounds with $abpy^{\bullet -}$ as a rather persistent anion radical ligand [67]. Although these species can be studied via the spectroelectrochemical response of their vibrational and electronic absorption bands, the additional information from EPR spectroscopy has been rather useful.

The anion radical $abpy^{\bullet -}$ and many of its complexes display rather poorly resolved EPR spectra (cf. Fig. 7) [19,24,25,34,36,46]. This phenomenon is similarly

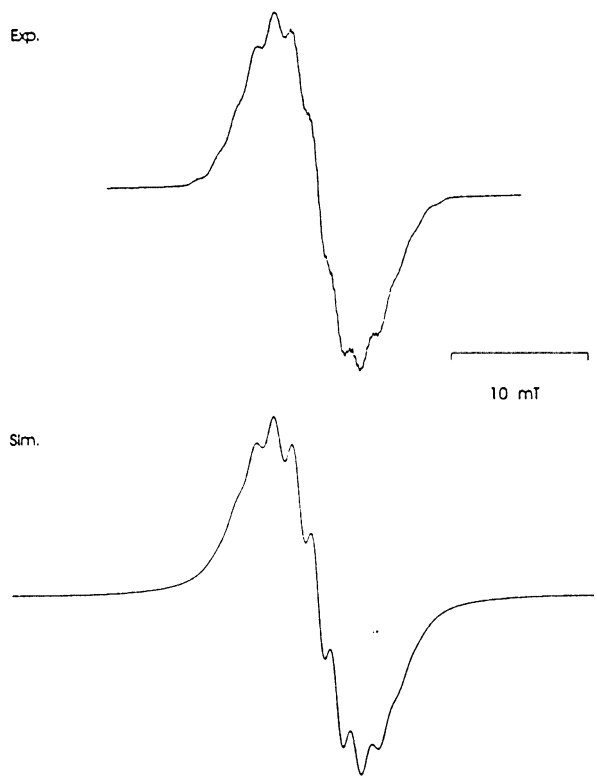

Fig. 7. X-band EPR spectrum of $\{(\mu\text{-abpy})[Cu(Ph_2P(CH_2)_5PPh_2)]_2\}^{\bullet +}$ in CH_2Cl_2/0.1 M Bu_4NPF_6 (top); computer simulated spectrum with $a(^{63}Cu) = 1.30$ mT, $a(^{65}Cu) = a(^{31}P) = 1.39$ mT (bottom) [46a].

known for the azobenzene anion radical [68] and is attributed to pronounced anisotropic line broadening, i.e. insufficient averaging of contributions from the **g** and **A** tensors, caused by the large concentration of spin at the two central ^{14}N nuclei of the azo group [68]. This effect is further compounded by the coordination of metal centers, which render the complexes less mobile in solution (decrease of the rotational correlation time). However, despite this unfavorable situation the following information could be extracted for complexes of $abpy^{\bullet -}$:

Electron-nuclear double resonance (ENDOR) spectroscopy of the dimolybdenum(0) complex $\{(\mu\text{-abpy})[Mo(CO)_4]_2\}^{\bullet -}$ yielded very small coupling constants for protons $H^{4,4'}$ and $H^{6,6'}$, values of 0.186 mT for $H^{3,3'}$ 0.255 mT for $H^{5,5'}$, and 0.24 mT for N_{py}, and, by implication from the total EPR linewidth, a hyperfine splitting of about 0.6 mT for the azo ^{14}N centers [24]. These data are in good agreement with the calculated HMO π spin populations [24]; they also illustrate how extensive hyperfine splitting from the nuclei in the 2-pyridyl rings contributes to the overall poor resolution of the EPR spectra of $abpy^{\bullet -}$-containing complexes.

The EPR/ENDOR data [24] confirm the above-mentioned notion that the four nitrogen centers comprise about two-thirds of the LUMO (the singly occupied MO, SOMO, of the radical species). Through ligand-to-metal spin polarization, this strong contribution from the coordinating π centers can cause rather large hyperfine coupling from suitable coordinated metal isotopes, i.e. isotopes with non-zero nuclear spin, sufficient natural abundance, and a relatively high magnetic moment for detection of EPR hyperfine interaction. Such isotopes include $^{63,65}Cu$ (69.2 and 30.8%, $I = 3/2$), $^{99,101}Ru$ (12.7 and 17.0%, $I = 5/2$), $^{185,187}Re$ (37.4 and 62.6%, $I = 5/2$), and ^{189}Os (16.1%, $I = 3/2$). Metal isotope coupling constants $a > 0.7$ mT have thus been observed for the corresponding radical complexes $[(abpy)Ru(bpy)_2]^{\bullet +}$ [19], $\{(abpy)[Re(CO)_3Cl]_{1\text{ or }2}\}^{\bullet -}$ [25,31,33], $\{(\mu\text{-abpy})[OsCl(C_6Me_6)]_2\}^{\bullet +}$ [44] and $\{(\mu\text{-abpy})[Cu(PR_3)_2]_2\}^{\bullet +}$ [46]. Comparison of the rhenium(I) species with a number of related mononuclear and dinuclear analogues [25,33,69] shows that the $^{185,187}Re$ hyperfine splitting of about 2.5 mT for the abpy systems is unusually large. Incidentally, the ^{95}Mo-NMR spectroscopic result for $(abpy)Mo(CO)_4$ (deshielding in comparison with related compounds) also confirms the strongly electron-accepting characteristics of the abpy ligand [27].

An additional parameter for investigating the electronic structure of radical complexes is the g factor [67]. The deviation of g(radical complex) from g(electron) = 2.0023 or from the value $g(abpy^{\bullet -}) = 2.0044$ of the free ligand radical anion [24] depends on the degree of metal–ligand (SOMO) mixing, on the spin–orbit coupling of the metal, and on the orbital ordering that determines the sign of the g shift [67]. Dinuclear chromium, molybdenum and tungsten tetracarbonyl complexes of $abpy^{\bullet -}$ thus exhibit isotropic g factors of 2.0040, 2.0050 and 2.0089, respectively [24]. The g anisotropy as measured of a glassy frozen solution is another measure for heavy metal participation at the SOMO. The numbers of $g_1 = 1.9782$, $g_2 = 1.9631$ and $g_3 = 1.9155$ for $\{(\mu\text{-abpy})[OsCl(C_6Me_6)]_2\}^{\bullet +}$ as determined by high-field EPR (W band, 95 GHz [44]) confirm the postulated high degree

of mixing between the metal d orbitals and the b_g MO of the abpy ligand. The effect of spin–orbit coupling alone is illustrated within the series $\{(\mu\text{-abpy})[M(bpy)_2][M'(bpy)_2]\}^{*3+}$, where the total g anisotropy g_1-g_3 increases from 0.0440 (M,M′ = Ru) via 0.1640 (M = Ru, M′ = Os) to 0.2510 (M,M′ = Os) [43]. In the absence of heavy metals from the second or third row of the periodic table, EPR studies at high fields and frequencies can help to confirm the ligand localization of the spin as illustrated in Fig. 8 for a stable ($abpy^{\bullet -}$)-bridged dicopper(I) species.

A remarkable phenomenon has been observed for the one-electron reduction products of the three isolated isomers of $[(abpy)_2Ru(bpy)]^{2+}$ [41]: whereas the *ctc* and *ccc* isomers (Fig. 2) show the typically [36] unresolved but nevertheless room temperature-detectable EPR signal at g fractionally lower than 2, the *cct* isomer with the predominantly spin-accommodating azo functions in the *trans* position (Fig. 9) exhibit severe line-broadening above 200 K, rendering its detection at ambient temperatures impossible [19,41]. This behavior suggests a slow-exchange situation for the electron hopping between the two equivalent abpy sites in complexes $[(abpy)_2Ru(bpy)]^{*+}$, which proves to be unusually configuration-dependent.

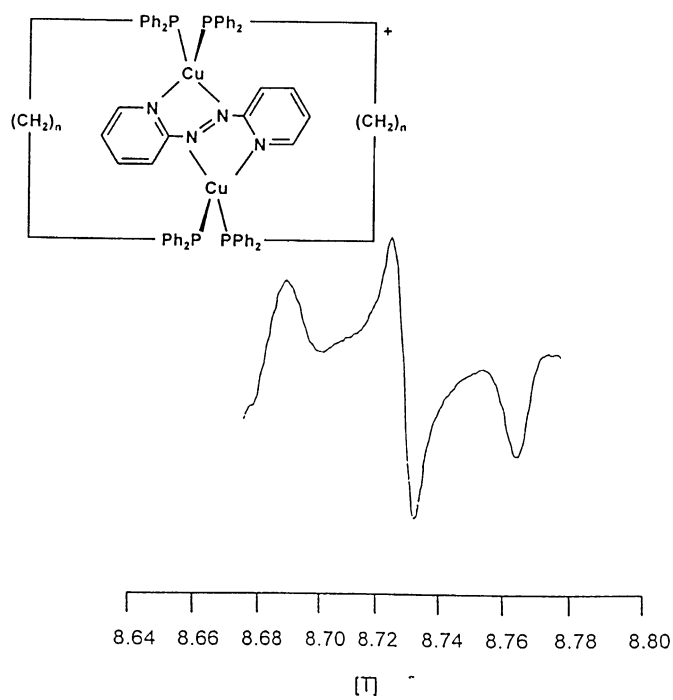

Fig. 8. EPR spectrum (245 GHz) of $\{(\mu\text{-abpy})[Cu(Ph_2P(CH_2)_6PPh_2)]_2\}(BF_4)$ in acetone–ethanol (5:1) at 5 K: $g_1 = 2.0134$, $g_2 = 2.0047$, $g_3 = 1.9968$ [46b].

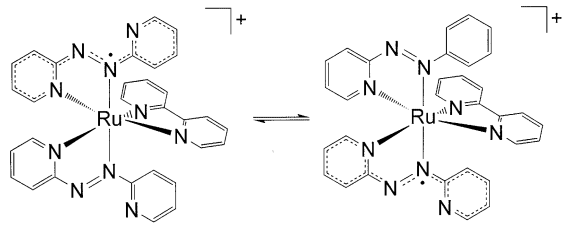

Fig. 9. Electron hopping in *cct*-$[(abpy)_2Ru(bpy)]^{\bullet +}$.

8. Complexes with S-frame ligands related to abpy

Coordinatively employed modifications of 2,2′-azobispyridine include the 3,3′- and 4,4′-isomers [3,10,20,70–72]. The 4,4′-azobispyridine ligand has been used as a bis(monodentate) bridge e.g. between tungsten(0) [10,70], ruthenium(II) [71], rhenium(I) [72] or osmium carbonyl cluster fragments [10]. HMO calculations, cyclic voltammetry, UV–Vis–IR spectroscopy and EPR studies of the reduced form $\{(\mu\text{-}4,4'\text{-abpy})[W(CO)_5]_2\}^{\bullet -}$ suggested bonding through the pyridyl nitrogen atoms [70] before a corresponding structure became available [10]; $[(H_3N)_5Ru]^{n+}$ and $[(OC)_3(bpy)Re]^{+}$ are coordinated similarly [71,72]. Intramolecular metal–metal interaction as a function of the ligand redox state [71] and photophysical properties [72] have been studied.

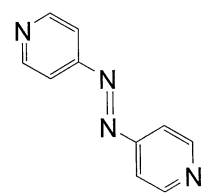

4,4´-abpy

Azo compounds with other, more complex metal-binding functions as substituents at the N=N group have been synthesized in the form of 2,2′-azobis(5-chloropyrimidine) (abcp) [73,74], 4,4′-azobis(2,2′-bipyridine) [75] and as various C-substituted azodicarbonyl species adc-R.

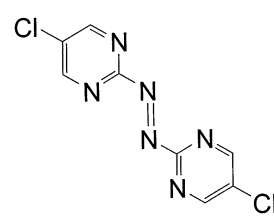

abcp

The abcp molecule was recently obtained through chlorinating oxidative coupling of 2-aminopyrimidine [73,74]. Its reduction potential is even lower than that of abpy by about 0.45 V. Reaction with excess $[Cu(PPh_3)_4](BF_4)$ produced not the expected diamagnetic dication but, instead, the radical complex $\{(\mu\text{-abcp})[Cu(PPh_3)_2]_2\}^{\bullet +}$ as mono-hexafluorophosphate [73]. The positively shifted redox potential at $+0.06$ V versus ferrocene/ferrocenium in CH_2Cl_2 is strong evidence for the tendency of the system to prefer the radical cation instead of the dicationic state. The structure of this unusually stable radical complex revealed a considerably lengthened N–N distance of 1.345 Å as compared with the 1.230 Å of the free ligand (Table 2) [73]. The 1.345 Å value signifies a bond order of 1.5 between typical N=N double bonds of about 1.23 Å and N–N single bonds of ca. 1.42 Å (Table 2). The absorption and EPR data (X- and W-band [73,74]) are also compatible with a $Cu^{I}(abcp^{\bullet -})Cu^{I}$ description of the system; other dinuclear species, including a dirhenium(I) radical complex, have been obtained [74].

The 4,4′-azobis(2,2′-bipyridine) ligand was devised to bind two $[(bpy)_2Ru]^{2+}$ fragments and then function as a reversibly redox-responsive molecular switch, modulating electron localization in the excited state, which can be detected via the emission intensity [75].

Table 2
Distances d (Å) in complexes of abpy and related ligands

Compound	d(NN)	$d(N_{azo}M)$	d(XM) [a]	d(MM)
$(abpy)SnBr_2Me_2$ [47]	1.229(22)	2.585(17)	2.793(18) [b]	–
abcp [74]	1.230(2)	–	–	–
abpy [18]	1.246(2)	–		–
$\{(\mu\text{-abpy})[Cu(PPh_3)_2]_2\}(BF_4)_2$ [26]	1.248(11)	2.095(6)	2.101(6)	4.937
$(abpy)Re(CO)_3Cl$ [31]	1.272(9)	2.143(5)	2.145(6)	–
$(abpy)Mo(CO)_4$ [26]	1.278(3)	2.190(2)	2.197(2)	–
ctc-$(abpy)_2RuCl_2$ [40]	1.267(9)	1.967(4)	2.025(7)	–
	1.294(9)	1.995(7)	2.023(6)	–
[*mer*-$(abpy)_3Ru](PF_6)_2$ [40]	1.274(8)	2.036(5)	2.068(6)	–
	1.282(7)	2.047(5)	2.062(5)	
	1.284(9)	2.047(5)	2.061(6)	
ctc-$(abpy)_2OsCl_2$ [43]	1.281(2)	2.024(2)	2.051(1)	–
	1.300(2)	1.958(2)	2.023(1)	–
$(\mu\text{-abpy})[Re(CO)_3Cl]_2$ [31]	1.304(10)	2.134(6)	2.135(5)	5.033(7)
$\{(\mu\text{-abcp})[Cu(PPh_3)_2]_2\}(PF_6)$ [73]	1.345(7)	2.043(3)	2.096(3)	4.866(1)
$\{(\mu\text{-adc-O}^{t}Bu)[Cu(Ph_2P(CH_2)_6PPh_2)]_2\}(BPh_4)$ [82] [c]	1.246(31)	2.050(15)	2.324(17)	4.828(3)
	1.308(26)	2.007(13)	2.316(14)	4.819(3)
$(adc\text{-Ph})Pt(PPh_3)_2$ [76]	1.401(9)	2.047(6)	2.016(5)	–
$(adc\text{-Ph})MoO(S_2CNMe_2)_2$ [77]	1.418(14)	2.119(18)	2.054(14)	–
$(adc\text{-O}^{i}Pr)Pt(PPh_3)_2$ [78]	1.421(6)	2.050(5)	2.027(4)	–

[a] X = N (abpy, abcp) or O (adc-R).
[b] Other pyridyl-N bond to tin(IV) at 2.899(17) Å.
[c] Two crystallographically different molecules in the unit cell.

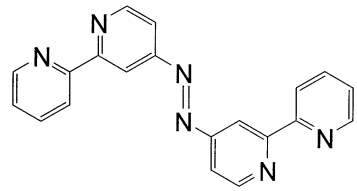

Azodicarbonyl ligands (adc-R) are available as donor-substituted species (R = NR_2 and OR) or, in hydrogenated form, as diacyl hydrazines (R = alkyl and aryl). Evidently, the conjugation of the low-lying π*(CO) MOs with π*(NN) creates an extremely strong electron acceptor situation, leading to a two-step redox system $(adc\text{-}R)^{0/\bullet -/2-}$ with strong π conjugation and a resonance-stabilized dianionic state (Scheme 8).

The adc-R ligands are even more attractive than abpy for coordination chemistry because just four of the six π centers can bind two metal atoms while the remaining two carbon π centers carry substituents R for tuning the electronic properties of the ligand.

As a consequence of the strong electron accepting capability of adc-R, isolated mononuclear [76–79] or dinuclear [59,80–84] metal complexes of the adc-R ligands are only known with $(adc\text{-}R)^{\bullet -}$ or $(adc\text{-}R)^{2-}$ forms.

Mononuclear compounds of $(adc\text{-}X)^{2-}$ have been structurally characterized with platinum and molybdenum complex fragments (Table 2) [76–78]. The N–N distances clearly point to a single bond and the short M–O bond lengths also confirm a formulation as depicted in Scheme 9.

The only structurally characterized dinuclear complex is that of {(μ-adc-O′Bu)[$Cu(Ph_2P(CH_2)_6PPh_2)$]$_2$}(BPh_4) with a metal–metal distance of about 4.82 Å (Table 2) [82]. This and related species were obtained by the reaction of copper powder, $Ph_2P(CH_2)_nPPh_2$ (or PR_3) and adc-O′Bu in wet methanol under air [81,82]

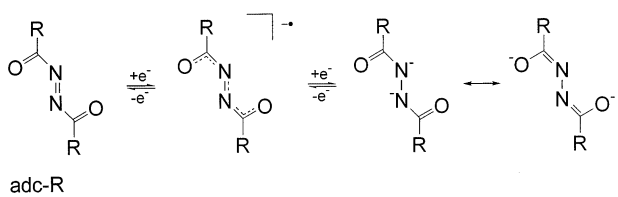

Scheme 8.

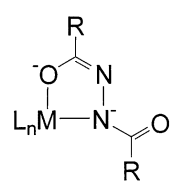

Scheme 9.

and eventual precipitation with $NaBPh_4$. According to the crystal structure (Fig. 10, Table 2) and the EPR data at 9.5 GHz (hyperfine structure [81]) and 245 GHz (g anisotropy [46b]) the stable, deep blue compound must still be formulated as an $Cu^{I}(adc^{\bullet -})Cu^{I}$ radical system. Nevertheless, the combination of unusually large metal coupling and high EPR resolution allowed us to detect separate $^{63}Cu^{63}Cu$, $^{63}Cu^{65}Cu$ and $^{65}Cu^{65}Cu$ combination lines [81]. Interestingly, the diphosphine ligands $Ph_2P(CH_2)_6PPh_2$ do not form nine-membered ring chelates but act as additional bridges (Scheme 10), thereby creating an 'inverse cryptate' situation with two metals as bridgeheads and an encapsulated organic radical ion (Fig. 10) [54,82].

Both the steric shielding and the large stability range of 1.16 V for the $\{(\mu\text{-adc-O}^{t}\text{Bu})[Cu(Ph_2P(CH_2)_6PPh_2)]_2\}^{\bullet +}$ intermediate contribute to the stability. Of the neighboring diamagnetic oxidation states (Scheme 11) the yellow $(\mu\text{-adc-O}^{t}\text{Bu})[Cu(Ph_2P(CH_2)_6PPh_2)]_2$ could be isolated whereas the labile $\{(\mu\text{-adc-O}^{t}\text{Bu})$-

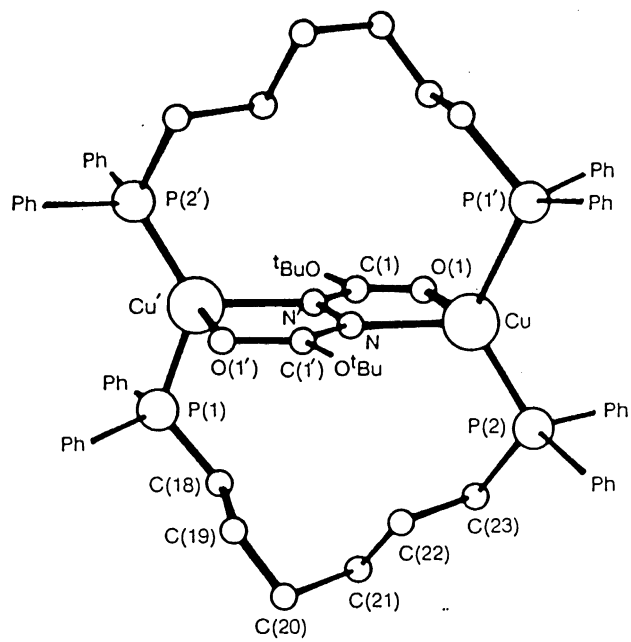

Fig. 10. Inverse cryptate structure of $\{(\mu\text{-adc-O}^{t}\text{Bu})[Cu(Ph_2P(CH_2)_6PPh_2)]_2\}^{\bullet +}$.

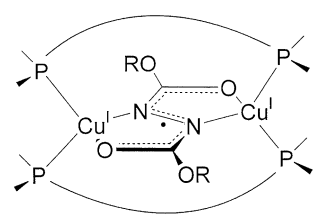

Scheme 10.

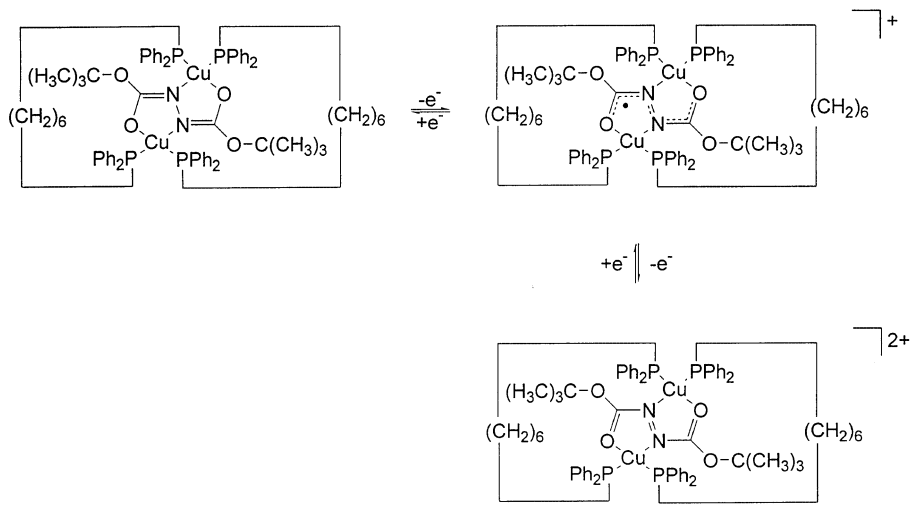

Scheme 11.

$[Cu(Ph_2P(CH_2)_6PPh_2)]_2\}^{2+}$ was only characterized UV–vis spectroelectrochemically with a longer-wavelength MLCT feature than the radical complex (725 nm) [82].

Whereas the ions $\{(\mu\text{-adc-R})[Cu(PR_3)_2]_2\}^{\bullet+}$ are clearly radical species as is an EPR-spectroscopically characterized (adc-O^{t}Bu)-bridged dirhenium(I) species [85], the corresponding systems $\{(\mu\text{-adc-R})[M(bpy)_2]_2\}(PF_3)_3$, M = Ru or Os, are better described as $M^{II}M^{III}$ mixed-valent species [59,80,83,84].

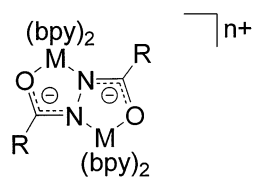

Arguments for the $M^{II}(\mu\text{-adc-R})^{2-}M^{III}$ versus the $M^{II}(\mu\text{-adc-R})^{\bullet-}M^{II}$ formulation are the smaller electrochemical potential range $\Delta E < 0.6$ V of these intermediates than that of the dicopper complexes ($\Delta E > 1.0$ V), the intense long-wavelength absorptions in the near infrared (> 1200 nm, inter-valence charge transfer), the observation of two different metal features in the XPS spectra (valence-localized situation), the temperature dependence of the magnetism, and the EPR results [59,83,84]. Whereas the diosmium systems remain EPR silent even at 3.5 K [59,84], the diruthenium species are observable below about 50 K. In addition to this rapid relaxation the large g anisotropy is very indicative of a predominantly metal-centered SOMO [83]. Nevertheless, this donor-bridged version of a mixed-valent system (hole-exchange mechanism [17,59,84]) results in remarkable sensitivity of the g anisotropy on the substituents R. In agreement with the π donor function of the

bridging $(adc\text{-}R)^{2-}$ ligand, the anisotropy is largest with acceptor substituents such as 4-C_6H_4-COOR [83]. The donor function of the bridging ligand in these (3+) ions is also evident from the lower comproportionation constant K_c for the diosmium case relative to the diruthenium system [59], quite in contrast to what is observed for acceptor-bridged mixed-valent dimers such as the Creutz–Taube ion and related species [84,86] such as $\{(\mu\text{-abpy})[M(bpy)_2]_2\}^{5+}$ (Section 5) [43].

9. Outlook

The coordination chemistry of S-frame bridging ligands with a central azo group is still at an early stage. Ligands other than the readily available abpy and adc-R systems can be devised and synthesized as was recently shown with abcp [73]. Furthermore, Tables 1 and 2 illustrate that complexes of the early transition metals, of iron and of Group 10 metals are not well represented. Given the special structural and electronic features of these ligands such as small metal–metal distances and low-lying π* MOs with efficient overlap at the metal–ligand interface, there is potential for more stable radical species [73], mixed-valent compounds [8,83] and magnetically coupled systems [26]; like bis(pyridyl)pyrazines [86], these ligands may also serve as bis-bidentate linkers in oligonuclear dendritic molecules. Metal–ligand charge transfer or azo-based excited state properties deserve further attention, and, for possible catalytic uses, heterodinuclear species with ligand-coupled but differently active metal centers may be envisaged. Yet another line of research lies in the selective response of different isomers (see Fig. 2) to tumor cells via different binding to DNA sequences, as demonstrated recently for $(pap)_2RuCl_2$ [87]. Summarizing, multifunctional azo compounds continue to be attractive, promising ligands for the development of functional metal complexes.

Acknowledgements

Continued support from Deutsche Forschungsgemeinschaft (DFG), Volkswagenstiftung and Fonds der Chemischen Industrie is gratefully acknowledged. I also thank all the dedicated coworkers mentioned in those literature citations that refer to our own work. Special thanks are due to Dr Brigitte Schwederski and Mrs Angela Winkelmann for their contributions to preparing this article.

References

[1] D.A. Baldwin, A.B.P. Lever, R.V. Parish, Inorg. Chem. 8 (1969) 107.
[2] A. Kirpal, L. Reiter, Ber. Dtsch. Chem. Ges. 60 (1927) 664.
[3] P.J. Beadle, R. Grzeskowiak, Inorg. Nucl. Chem. Lett. 3 (1967) 245.
[4] P.-O. Åstrand, P.S. Ramanujam, S. Hvilsted, K.L. Bak, S.P.A. Sauer, J. Am. Chem. Soc. 122 (2000) 3482.
[5] A. Natansohn (Ed.), Azobenzene-Containing Materials, Wiley-VCH, Weinheim, 1999.

[6] H. Zollinger, Color Chemistry: Syntheses, Properties and Applications of Organic Dyes and Pigments, Weinheim, VCH, 1991.
[7] (a) A. Albini, H. Kisch, Top. Curr. Chem. 65 (1976) 105. (b) H. Kisch, P. Holzmeier, Adv. Organomet. Chem. 34 (1992) 67. (c) D. Sellmann, A. Fürsattel, Angew. Chem. 111 (1999) 2142; Angew. Chem. Int. Ed. Engl. 38 (1999) 2023.
[8] M. Kurosawa, T. Nankawa, T. Matsuda, K. Kubo, M. Kurihara, H. Nishihara, Inorg. Chem. 38 (1999) 5113.
[9] S. Banerjee, S. Bhattacharyya, B.K. Dirghangi, M. Menon, A. Chakravorty, Inorg. Chem. 39 (2000) 6.
[10] W.-Y. Wong, S.-H. Cheung, S.-M. Lee, S.-Y. Leung, J. Organomet. Chem. 596 (2000) 36.
[11] R.A. Krause, Struct. Bonding (Berlin) 67 (1987) 1.
[12] M. Shivakumar, K. Pramanik, P. Ghosh, A. Chakravorty, J. Chem. Soc. Chem. Commun. (1998) 2103.
[13] M. Shivakumar, K. Pramanik, P. Ghosh, A. Chakravorty, Inorg. Chem. 37 (1998) 5968.
[14] W. Kaim, S. Kohlmann, Inorg. Chem. 26 (1987) 68.
[15] A. Haim, Prog. Inorg. Chem. 30 (1983) 273.
[16] O. Kahn, Molecular Magnetism, New York, VCH, 1993.
[17] W. Kaim, A. Klein, M. Glöckle, Acc. Chem. Res. 33 (2000) 755.
[18] H. Bock, R. Dienelt, H. Schödel, T.T.H. Van, Struct. Chem. 9 (1998) 279.
[19] M. Krejcik, S. Zalis, J. Klima, D. Sykora, W. Matheis, A. Klein, W. Kaim, Inorg. Chem. 32 (1993) 3362.
[20] R. Grzeskowiak, C. Whatley, M. Goldstein, Spectrochim. Acta Part A 31 (1975) 1577.
[21] A.J. Bellamy, I.S. MacKirdy, C.E. Niven, J. Chem. Soc. Perkin Trans. II (1983) 183.
[22] R.N. Goyal, Indian J. Chem. A 27 (1988) 858.
[23] S. Kohlmann, S. Ernst, W. Kaim, Angew. Chem. 97 (1985) 698; Angew. Chem. Int. Ed. Engl. 24 (1985) 684.
[24] W. Kaim, S. Kohlmann, Inorg. Chem. 25 (1986) 3442.
[25] W. Kaim, S. Kohlmann, Chem. Phys. Lett. 139 (1987) 365.
[26] W. Kaim, S. Kohlmann, J. Jordanov, D. Fenske, Z. Anorg. Allg. Chem. 598–599 (1991) 217.
[27] E.C. Alyea, J. Malito, S.D. Ernst, W. Kaim, S.J. Kohlmann, Polyhedron 8 (1989) 921.
[28] W. Kaim, S. Ernst, S. Kohlmann, Polyhedron 5 (1986) 445.
[29] W. Kaim, S. Ernst, S. Kohlmann, Chem. Unserer Zeit 21 (1987) 50.
[30] W. Kaim, S. Kohlmann, Inorg. Chem. 25 (1986) 3306.
[31] H. Hartmann, T. Scheiring, J. Fiedler, W. Kaim, J. Organomet. Chem. 604 (2000) 267.
[32] G.J. Stor, F. Hartl, J.W.M. van Outersterp, D. Stufkens, Organometallics 14 (1995) 1115.
[33] W. Kaim, S. Kohlmann, Inorg. Chem. 29 (1990) 2909.
[34] E. Wa1dhör, J. Poppe, W. Kaim, E. Cutin, M. Garcia Posse, N.E. Katz, Inorg. Chem. 34 (1995) 3093.
[35] S.D. Ernst, W. Kaim, Inorg. Chem. 28 (1989) 1520.
[36] W. Kaim, S. Ernst, V. Kasack, J. Am. Chem. Soc. 112 (1990) 173.
[37] S.I. Gorelsky, E.S. Dodsworth, A.B.P. Lever, A.A. Vicek, Coord. Chem. Rev. 174 (1998) 469.
[38] L.S. Kelso, D.A. Reitsma, F.R. Keene, Inorg. Chem. 35 (1996) 5144.
[39] S. Ernst, V. Kasack, W. Kaim, Inorg. Chem. 27 (1988) 1146.
[40] J. Fees, H.-D. Hausen, W. Kaim, Z. Naturforsch. B 50 (1995) 15.
[41] M. Heilmann, F. Baumann, W. Kaim, J. Fiedler, J. Chem. Soc. Faraday Trans. 92 (1996) 4227.
[42] P. Majumdar, A.K. Deb, S. Goswami, Proc. Indian Acad. Sci. Chem. Sci. 110 (1998) 21.
[43] (a) M. Heilmann, F. Baumann, W. Kaim, J. Fiedler, manuscript in preparation. (b) M. Heilmann, A.F. Stange, H.-D. Hausen, W. Kaim, unpublished results.
[44] F. Baumann, W. Kaim, G. Denninger, H.-J. Kümmerer, J. Fiedler, manuscript in preparation.
[45] S. Greulich, R. Reinhardt, J. Fiedler, W. Kaim, unpublished results.
[46] (a) M. Schwach, S. Kohlmann, W. Kaim, unpublished results. (b) A.-L. Barra, L.-C. Brunel, F. Baumann, M. Schwach, M. Moscherosch, W. Kaim, J. Chem. Soc. Dalton Trans. (1999) 3855.
[47] M. Camalli, F. Caruso, G. Mattogno, E. Rivarola, Inorg. Chim. Acta 170 (1990) 225.
[48] E. Rivarola, A. Silvestri, G. Alonzo, R. Barbieri, R.H. Herber, Inorg. Chim. Acta 99 (1985) 87.

[49] G. van Koten, K. Vrieze, Adv. Organomet. Chem. 21 (1982) 151.
[50] S. Greulich, W. Kaim, A. Stange, H. Stoll, J. Fiedler, S. Zalis, Inorg. Chem. 35 (1996) 3998.
[51] (a) M.J. Maroney, W.C. Trogler, J. Am. Chem. Soc. 106 (1984) 4144. (b) P. Overbosch, G. van Koten, A.L. Spek, G. Roelofsen, A.J.M. Duisenberg, Inorg. Chem. 21 (1982) 3908.
[52] E. Haselbach, Helv. Chim. Acta 53 (1970) 1526.
[53] C. Vogler, H.-D. Hausen, W. Kaim, S. Kohlmann, H.E.A. Kramer, J. Rieker, Angew. Chem. 101(1989) 1734; Angew. Chem. Int. Ed. Engl. 28 (1989) 1659.
[54] M. Schwach, H.-D. Hausen, W. Kaim, Chem Eur. J. 2 (1996) 446.
[55] A. Bencini, I. Ciofini, C.A. Daul, A. Ferretti, J. Am. Chem. Soc. 121 (1999) 11 418.
[56] M. Hidai, Y. Mizobe, Chem. Rev. 95 (1995) 1115.
[57] J. Rall, M. Wanner, M. Albrecht, F.M. Hornung, W. Kaim, Chem. Eur. J. 5 (1999) 2802.
[58] A. Klein, S. Hasenzahl, W. Kaim, J. Fiedler, Organometallics 17 (1998) 3532.
[59] W. Kaim, V. Kasack, Inorg. Chem. 29 (1990) 4696.
[60] M. Ladwig, W. Kaim, J. Organomet. Chem. 419 (1991) 233.
[61] M. Ladwig, W. Kaim, J. Organomet. Chem. 439 (1992) 79.
[62] W. Kaim, R. Reinhardt, M. Sieger, Inorg. Chem. 33 (1994) 4453.
[63] (a) U. Kölle, M. Grätzel, Angew. Chem. 99 (1987) 572; Angew. Chem. Int. Ed. Engl. 26 (1987) 568. (b) U. Kölle, B.-S. Kang, P. Infelta, P. Compte, M. Grätzel, Chem. Ber. 122 (1989) 1869.
[64] C. Craix, S. Chardon-Noblat, A. Deronzier, R. Ziessel, J. Electroanal. Chem. 362 (1993) 301.
[65] A.A. Vlcek, Coord. Chem. Rev. 43 (1982) 39.
[66] E. Dodsworth, A.B.P. Lever, Inorg. Chem. 29 (1990) 499.
[67] W. Kaim, Coord. Chem. Rev. 76 (1987) 187.
[68] C.S. Johnson, R. Chang, J. Chem. Phys. 43 (1965) 3183.
[69] A. Klein, C. Vogler, W. Kaim, Organometallics 15 (1996) 236.
[70] (a) W. Kaim, S. Kohlmann, Inorg. Chem. 29 (1990) 1898. (b) W. Kaim, S. Kohlmann, S. Ernst, B. Olbrich-Deussner, C. Bessenbacher, A. Schulz, J. Organomet. Chem. 321 (1987) 215.
[71] J.-P. Launay, M. Tourrel-Pagis, J.-F. Lipskier, V. Marvaud, C. Joachim, Inorg. Chem. 30 (1991) 1033.
[72] V.W.-W. Yam, V.C.-Y. Lau, L.-X. Wu, J. Chem. Soc. Dalton Trans. (1998) 1461.
[73] N. Doslik, T. Sixt, W. Kaim, Angew. Chem. 110 (1998) 2125; Angew. Chem. Int. Ed. Engl. 37 (1998) 2403.
[74] N. Doslik, W. Kaim, T. Sixt, S. Zalis, J. Fiedler, H.-J. Kümmerer, G. Denninger, manuscript in preparation.
[75] J. Otsuki, K. Sato, M. Tsujino, N. Okuda, K. Araki, M. Seno, Chem. Lett. (1996) 847.
[76] S.D. Ittel, J.A. Ibers, Inorg. Chem. 12 (1973) 2290.
[77] C.P. Marabella, J.H. Enemark, W.E. Newton, J.W. McDonald, Inorg. Chem. 21 (1982) 623.
[78] D. Chan, L. Cronin, S.B. Duckett, P. Hupfield, R.N. Perutz, New J. Chem. (1998) 511.
[79] G. Avar, W. Rüsseler, H. Kisch, Z. Naturforsch. B 42 (1987) 1441.
[80] W. Kaim, V. Kasack, H. Binder, E. Roth, J. Jordanov, Angew. Chem. 100 (1988) 1229; Angew. Chem. Int. Ed. Engl. 27 (1988) 1174.
[81] W. Kaim, M. Moscherosch, J. Chem. Soc. Faraday Trans. 87 (1991) 3185.
[82] M. Moscherosch, J.S. Field, W. Kaim, S. Kohlmann, M. Krejcik, J. Chem. Soc. Dalton Trans. (1993) 211.
[83] V. Kasack, W. Kaim, H. Binder, J. Jordanov, E. Roth, Inorg. Chem. 34 (1995) 1924.
[84] V. Kasack, W. Kaim, J. Jordanov, E. Roth, unpublished results.
[85] K.S. Chen, J.K.S. Wan, J. Am. Chem. Soc. 100 (1978) 6051.
[86] M. Marcaccio, F. Paolucci, C. Paradisi, S. Roffia, C. Fontanesi, L.J. Yellowlees, S. Serroni, S. Campagna, G. Denti, V. Balzani, J. Am. Chem. Soc. 121 (1999) 10 081.
[87] A.H. Velders, H. Kooijman, A.L. Spek, J.G. Haasnoot, D. de Vos, J. Reedijk, Inorg. Chem. 39 (2000) 2966.